



## SEISMIC DESIGN OF BRIDGE PIERS WITH STIFFENED BOX SECTIONS USING LP PLATES

Tatsumasa TAKAKU<sup>1</sup>, Yuhshi FUKUMOTO<sup>2</sup>, Tetsuhiko AOKI<sup>3</sup> and K.A.S.SUSANTHA<sup>4</sup>

### SUMMARY

Bridge piers with a low structural indeterminacy need to have enough strength and ductility to absorb amounts of seismic energy. It is one of the solution to use Longitudinally Profiled Steel Plate (LP plate) for flanges and webs rather than plates of uniform thickness, allowing a better fitting of the bending moment distribution resulting from the applied loading, and thus also a larger spread of the plate yielding. Based upon the results of a series of experimental and analytical studies, this paper presents structural design recommendations for bridge piers with LP plates. Feasibility study is proposed both in strength and ductility, then in economy in the aspect of cost saving views. Design flow is just the same as that of piers with uniform thickness, initially with uniform thickness, then replacing them by LP plates. This paper describes following items: (1) Fundamental knowledge of beam-column with LP plates based upon a series of testing and analytical works, mainly done in the laboratory of Aichi Institute of Technology; (2) Performance assessment of them, using test mainly conducted in the laboratory of Fukuyama University; and (3) Design and FEM analysis of a rigid frame pier using the testing model followed by a proposal for the application of LP plates to bridge piers using a few case studies.

### INTRODUCTION

When bridge piers are subjected to a big earthquake, local buckling occurs at the critical sections near the bottom of piers or at the stepwise changes in the wall thickness. Since then, focus is on the critical section and the vicinity of the basement. The Japanese Specification [1] recommends a specific filling height of concrete in box section to prevent the buckling modes, or more tough sections to ensure sufficient strength and ductility. The linearly tapered rolled plates are sometimes used for flanges of bridge main girders. It allows a better fitting of the bending moment distribution due to applied loading. In the case of beam-column problems, tapered plates are considered to allow much more effective behavior with a good design.

---

<sup>1</sup> Director, Toko Consultants Co., Ltd., Tokyo, Japan. Email: takakut@tokoc.co.jp

<sup>2</sup> Professor, Dept. of Civil and Environmental Eng., Fukuyama University, Fukuyama, Japan. Email: fukumoto@fucc.fukuyama-u.ac.jp

<sup>3</sup> Professor, Dept. of Civil Eng., Aichi Institute of Technology, Toyota, Japan. Email: aoki@aitech.ac.jp

<sup>4</sup> Research staff, Dept. of Civil Eng., Aichi Institute of Technology, Toyota, Japan. Email: susantha@aitech.ac.jp

The use of LP plates leads to cost saving in material and in connections without filler plates. Application of LP plates for highway bridge girders [2] and ship girders can be found everywhere in Japan and are totally counted as 13000 ton steel weight of existing structures in 1999 since 1993 [3]. Based upon the experiences of the girders, application of LP plates can be extended to the beam-column problems. Since 2000, a number of laboratory tests have been carried out by the universities [4~9], industry and the associations (e.g., Japan Association of Steel Bridge Construction [10]). Beam-column is subjected both to thrust and bending moment at the same time so that LP plates show different behavior in plastic region whereas girders with LP plates is designed for bending moment only in elastic region. A rigid frame pier with LP plates is subjected to earthquake in two directions, longitudinally and transversely. Application of LP plates to the bridge piers is considered to be a 3-dimensional problem subjected to combined forces of bending moment, shear and thrust in two directions, which leads to a more complicated and sophisticated engineering problem.

## FUNDAMENTALS OF BEAM-COLUMN WITH LP PLATE

### LP Steel and its Effectiveness

LP steel plate is manufactured in prescribed form controlling pressure and speed of rollers in rolling process.

Typical LP steel shapes produced in Japan are shown in Fig. 1. Past history of rolling process makes difference in the mechanical properties between thick and thin sides of the plate as explained below.

1) Yield strength: the thin side of the plate shows higher yield strength due to faster cooling and suffering stronger rolling pressure.

2) Tensile strength and elongation: The thinner the plate thickness, the higher the tensile strength and the lesser the elongation.

The above mechanical properties can be moderated by more fine control of rolling and heat-treating. Merit of usage of LP plate is to reduce the total weight of steel material, no use of filler plate at the connection between two different thickness plates and relaxing stress concentration at the connection. On the other hand, cost increasing factors and some difficulty in cutting and manufacturing of LP part are considered to be additional concerns. The feasibility study of LP steel plate is focused on the following two points: (1) Economy: Balance between steel weight reduction effect and additionally increased cost for the LP plate; (2) Advancement of seismic resistance performance: Advances of strength and ductility.

### General Design Details for High Ductility

For box shaped piers using LP steel plates, care should be taken to preserve certainly horizontal sustaining force in the plastic deformation. Following points are worth to be considered in this regard:

1) Retain of continuity of the cross sectional rigidity: Design members not to have the discontinuity lines such as ends of the tapered plate, ends of constant part of the plate followed by tapered plate, welding lines, upper surface line of filled-concrete, and discontinuity position of the cross section, at the same position.

2) Prevention of stress concentration due to local buckling and reduction of P- $\delta$  effect: LP plate has the effect of reducing stress concentration at local points, because LP plate changes continuously the rigidity

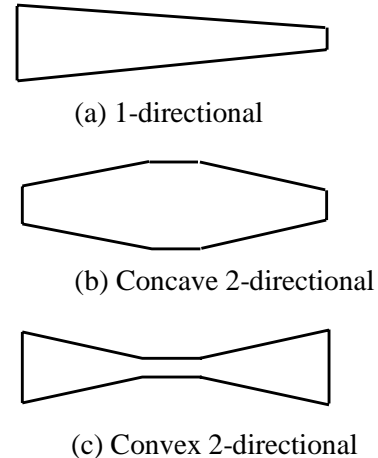


**Fig. 1 Typical LP Steel Plates**

of cross section of the member. Use of thicker plate at the locations where maximum stress occurs due to the external forces reduces secondary deformation ( $P-\delta$  effect) and contributes to enlarge the plastic region and ductility.

3) Corresponding to bi-directional seismic forces in longitudinal and transverse directions of bridge axis, LP plates are to be used both for the flange and web. As for the flange effect, bending stress is reduced due to the tapering along with the bending moment gradient. For the web, shear is resisted and the axial stress is reduced resulting delay in the initiation of flange buckling.

4) The height of filled-concrete and the length of taper plates are designed such that the yield strength by the horizontal force or horizontal resisting force determined from the local buckling exceeds the horizontal resisting force at rupture section (base section). The height of filled-concrete  $h_c$  is determined to satisfy the following condition [1].

$$h_c > \left(1 - M_{ys} / M_a\right) \cdot h \quad (1)$$

where  $M_{ys}$ , and  $M_a$  are the elastic limit moments, modified to include the effect of axial compression at the top and bottom sections of the tapered portion of the column, respectively, and  $h$  is the height from the base to the center of the earthquake force.

### Mold Line of LP Plates for Box Column

Setting of mold line of LP plates is the first process to be determined by the designer, which may affect both on buckling mode and ultimate strength of the member. Three different types of mold line setting of the plate, namely outside taper, central taper, and inside taper, are demonstrated in Figs. 2(a) to (c). The special features of each type are explained as:

- (a) Outside Taper: The bending rigidity of the cross section is the largest among the three types. The secondary bending at the infection point ( $P-\delta$  effect) is large. It is easy to allocate inside ribs and diaphragms.
- (b) Central taper: Inclination of the plate appears on both sides of the central plane of the member. The secondary bending at the infection point becomes small.
- (c) Inside taper: The bending rigidity of the cross section is the smallest among the three types. There is a large secondary bending at the infection point. A variable height of ribs should be used.

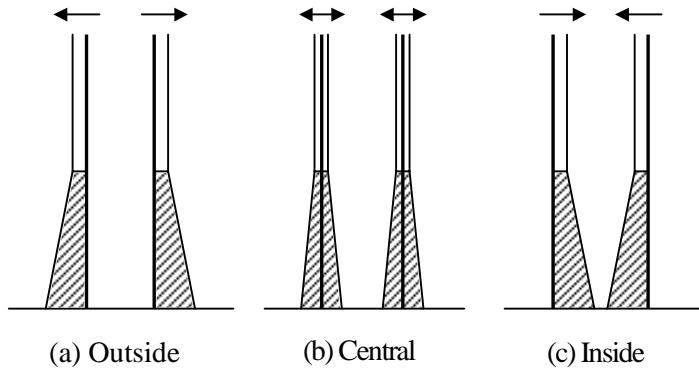


**Fig. 2 Mold Lines of LP Plates**

In order to investigate the effects of above three types of mold line setting together with their tapering ratio, eight specimens were tested [8]. The details of the test program are listed in Table 1. Cyclic loading test results of these three types of mold lines (i.e., Specimen Set-1) are exhibited in Fig. 3. Followings key observations are made from the test:

- 1) Maximum load and ductility ratio of specimen with outside taper are 4 to 5% higher than those of others.

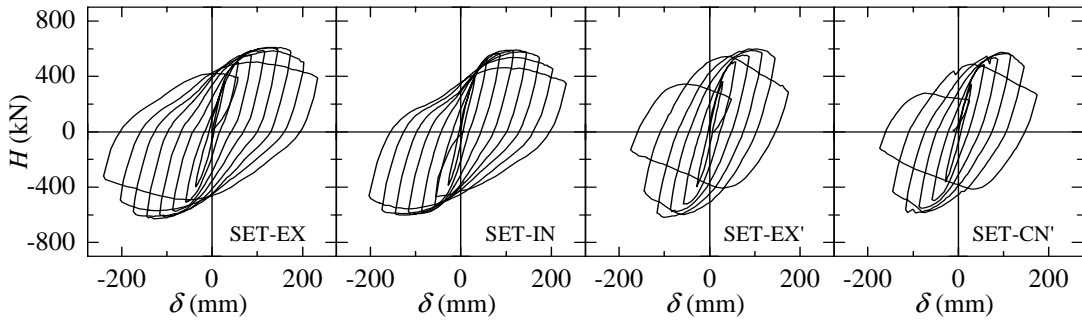


**Fig. 3 Horizontal Load-Horizontal Displacement Relations**

- 2) No eccentric axial load presents in specimen with central taper. Therefore, the effect of secondary bending at the infection point ( $P-\delta$  effect) does not exist.
- 3) Column with outside taper is identified as the most advantageous from the point of section performance and manufacturing.

#### Tapering Ratio and Failure Mode

If one chooses improper tapering ratio, plate buckling might occur locally and the strength and ductility may be reduced. Therefore, tapering ratio should be determined carefully, so that buckling occurs over whole range of tapered part. Tapering ratio is defined by two methods namely: (1) General definition; and (2) Conventional method.

- 1) General definition [4],

$$\eta = \frac{h}{h_{LP}} \left( 1 - \frac{M_{ycU}}{M_{ycL}} \right) \quad (2)$$

where  $M_{ycU}$  and  $M_{ycL}$  are the elastic limit moments, modified to include the effect of axial compression at the top and bottom sections of tapered portion of the column.

**Table 1 Details of Test Specimens**

Steel Grade	SM490A ( $\sigma_y=314$ MPa)		
Width of section, $b$ (mm)	450~458		
Thickness of plates, $t$ (mm)	6~10		
Width of ribs, $b_s$ , (mm)	75		
Thickness of stiffeners, $t_s$ (mm)	9		
Height of column, $h$ (mm)	2343		
Specimen Set-1			
Name of Specimen	SET-EX SET-EX'	SET-CN'	SET-IN
Name of mold line	Outside taper	Central taper	Inside taper
Outer dimension	$b=450 \sim 454$	$b=450 \sim 452$	$b=450$
Specimen Set-2			
Name of tapering	STG08	STG10	STG12
Tapering ratio	$\alpha=0.8$	$\alpha=1.0$	$\alpha=1.2$
Height (mm)	1929	2343	2587
			2985

2) Conventional method [8],

$$\alpha = g/g_0 = (t_L - t_U)/(t_L^* - t_U^*) \quad (3)$$

where  $g_0$  is the tapering ratio where stress due to axial and bending becomes yield along the taper plate (adaptive taper ratio) having the thickness of the plate at upper and lower ends as  $t_U^*$  and  $t_L^*$ ;  $g = (t_L - t_U)/h_{LP}$  in which  $t_L$  and  $t_U$  are the thicknesses at lower and upper ends of the tapered plate, respectively, and  $h_{LP}$  is the length of the tapered plate.

#### *Relationship between two equations defining tapering ratio*

Consider, as a simple case, a rectangular cross section composed of four plates with thickness  $t$  and width  $b$ , and axial force ratio at the base given by  $P/Py=P^*$ . Then the section modulus  $Z$  becomes  $Z=(4/3)b^2t$  and  $M_{ycL}$  and  $M_{ycU}$  lead to

$$M_{ycL} = (1 - P^*)\sigma_y \cdot (4/3)b^2 t_L = (1 - P^*)\kappa t_L \quad (\kappa = \sigma_y \cdot (4/3)b^2) \quad (4)$$

$$M_{ycU} = (1 - P^* t_L / t_U) \kappa t_U \quad (5)$$

Introducing Eqs. (4) and (5) into Eq. (2),

$$\eta = \frac{h}{h_{LP}} \left( 1 - \frac{(1 - P^* t_L / t_U) t_U}{(1 - P^*) t_L} \right) = \frac{(t_L - t_U)}{h_{LP}} \cdot \frac{h}{t_L} C \quad C = 1/(1 - P^*) \quad (6)$$

when  $\eta=1$  in Eq. (2), the geometrical relations of  $M_{ycL}$  and  $M_{ycU}$  becomes linear as shown in Fig. 4. Then from Eq. (6)  $h/t_L^*$  can be expressed as

$$\frac{t_L^*}{h} = \frac{(1 - P^*) \kappa t_L - (1 - P^* t_L^* / t_U^*) \kappa t_U^*}{(1 - P^*) \kappa h_{LP}} = \frac{(t_L^* - t_U^*)}{h_{LP}} \cdot C \quad (7)$$

Introducing the tapering ratio in Eq. (3),  $g_0 = (t_L^* - t_U^*)/h_{LP}$ , into Eq. (7) leads to  $t_L^*/h = g_0 C$ . As a result, Eq. (3) can be expressed as

$$\alpha = \frac{g}{g_0} = \frac{(t_L - t_U)}{h_{LP}} \cdot \frac{h}{t_L^*} C \quad (8)$$

Comparing Eq. (8) with former Eq. (6), these two expressions are found to be the same except for the second term  $h/t_L$  or  $h/t_L^*$ . We usually choose  $t_L$  as  $t_L^*$  aiming at optimum design, so the  $\eta$  and  $\alpha$  have almost the same value.

In practical design procedures, the vertical load  $P$  and the horizontal load  $H$  are given first, then the adaptive section, that is the one with plate thickness  $t_U^*$  and  $t_L^*$ , which yields simultaneously at the upper and lower ends of the tapered plate, are decided as basis. The fundamental design value of the adaptive gradient of the tapered plate,  $g_0$  in Eq. (3), is then simply found to be  $g_0 = (t_L^* - t_U^*)/h_{LP}$  or alternatively

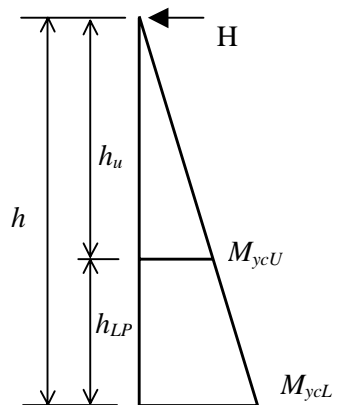


**Fig. 4 Relationship of  $M_{ycU}$  and  $M_{ycL}$  for  $\eta=1$**

$g_0 = (t_L^*/h)/C$ . Here, the physical meaning is clear and along with the design procedure, the definition of tapering ratio by Eq. (3),  $\alpha = g/g_0$ , may be more practicable. The value of  $\alpha$  greater than unity ( $\alpha > 1.0$ ) should be avoided, but  $\alpha = 0.9$  to 0.93 is recommended for the structures using tapered plates. Designers can easily understand the value of  $\alpha$  in those cases because the meaning of basic value of  $g_0$  is clear.

Three types of varying stress distributions along the taper plate using conventional definition are illustrated in Fig.5.

- 1) Positive gradient:  $\alpha < 1$ , ratio of change of plate thickness is gentle so that maximum stress appears at the bottom end of plate and yielding or occurrence of buckling delays at the boundary line between tapered and normal plates.
- 2) Adaptive taper ratio:  $\alpha = 1$ , stress distributes uniformly over whole range of the taper plate.
- 3) Negative gradient:  $\alpha > 1$ , ratio of change of plate thickness is so steep that the maximum stress occurs at the boundary line between tapered and normal plates and plate buckle there.

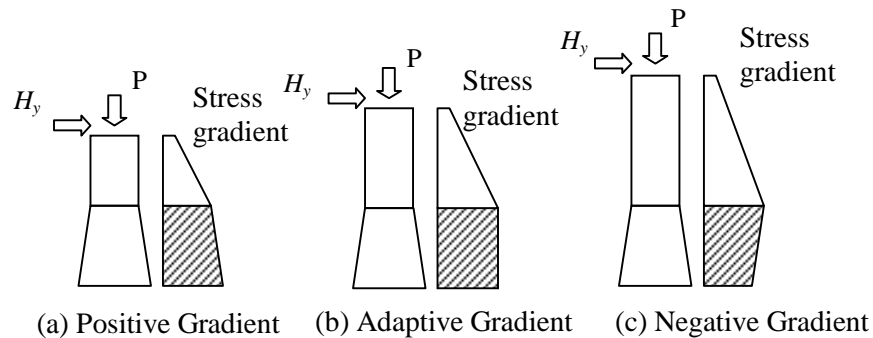


**Fig. 5 Three Types of Stress Distributions**

Following important points are observed from the cyclic test results of four specimens having different conventional tapering ratios as given in Table 1 (Specimen Set-2) [8]:

- 1) Tapering ratio  $\alpha$  has less effect on the maximum strength.
- 2) Ductility ratio: Specimen with the adaptive tapering ratio (specimen STG10) shows the largest ductility ratio. Comparing with the adaptive tapering ratio's specimen, one with the positive gradient (specimen STG08) shows 14% less value, negative ones (specimens STG12 and STG15) show 35% and 33% less values, respectively.
- 3) Specimen with positive gradient has higher ductility than that of negative gradient specimen and the buckling behavior is found to be similar with that of constant plate thickness.
- 4) In negative gradient specimen's, the maximum stress occurs at just upper part of the connecting line between LP and constant thickness plates, leading to a consequent local buckling at there. Therefore, caution needs to be taken not to have negative gradient in the design.
- 5) In order to spread the plastic region through whole range of LP, adaptive gradient is the best. Considering uncertainty in fabricating, external loading conditions, and minor changing in design, it may be recommended to use  $\alpha = 0.90 \sim 0.93$ , so that the local buckling at upper part of boundary line does not occur.

### Stiffeners and Rigidity

Ratio of rigidity ratio  $\gamma$  to required minimum rigidity ratio  $\gamma^*$ ,  $\gamma/\gamma^*$ , is recommended to be around 3.0 according to the elasto-plastic buckling tests under repeated loading that had been done so far. Cyclic loading tests have been conducted using three test specimens having different stiffeners rigidity [9]. The

section at mid height of the first panel from the bottom is used for calculating the stiffeners rigidity. The rigidity ratios  $\gamma/\gamma^*$  were selected as 2.2, 3.2 and 4.3 (i.e., specimens GAM22, GAM32, and GAM43, respectively), keeping thickness of stiffeners constant at 6 mm but changing their depth based on the following fundamental knowledge: (1)  $\gamma/\gamma^* = 2.2$  (GAM22): Rigidity ratio of stiffener is somewhat small; (2)  $\gamma/\gamma^* = 3.2$  (GAM32): Rigidity ratio of stiffener is proper; (3)  $\gamma/\gamma^* = 4.3$  (GAM43): Rigidity ratio of stiffener is somewhat large. Following conclusions are drawn from the test:

- 1) The maximum strength is expected in specimen GAM43 because it has the largest rigidity ratio. However, the strength of the column reduced immediately after the maximum load. The reason for this strength decrease is that the local buckling between ribs occurred easily and concentrated at the weakest point, even if the rigidity of stiffener increased to a significant level. This means that in such cases, the behavior of the pier with LP plate becomes similar to that of normal thickness plate columns. Comparing with specimen GAM32, the maximum strength of specimen GAM43 is almost the same but the ductility ratio decreases about 10%.
- 2) GAM22: The maximum strength of GAM22 decreases 5% and the ductility ratio decreases 10% comparing with those of specimen GAM32.
- 3) The rigidity ratios  $\gamma/\gamma^*$  of around 3.0 is recommended to be used.

### **Tapered Stiffeners**

Since rigidities calculated for the section composed by LP plates vary continuously, it is desirable to use stiffener also with varied cross section in order to keep the constant  $\gamma/\gamma^*$  ratio along the length of the member. In the case of stiffened LP plate in which stiffeners have constant cross section, overall buckling will occur at the region of small  $\gamma/\gamma^*$  ratio but local buckling at the region of large  $\gamma/\gamma^*$  ratio and it may not be expected expanding of the plastic region. Therefore, another set of specimens were tested to examine the effects of tapered stiffeners on the overall behavior of tapered plate columns [9]. The same type of LP plates as used in the flange plates are used for stiffeners as well. The main findings of the test are as follows:

- 1) When LP plate is used for the stiffeners too, whole rigidity of the stiffened plate will increase. Then the stress gradient changes to negative type. Design should be done carefully to avoid this phenomenon.
- 2) In the case of strongly positive stress gradient, LP effect will be disappeared and local buckling likely to occur at the bottom of the column.
- 3) By using LP plate for the stiffeners while controlling its height, stiffened plate with constant rigidity ratios  $\gamma/\gamma^*$  along the member can be designed.

## **PERFORMANCE ASSESSMENT AND LIMIT STATE OF DUCTILITY**

### **Tapering Ratio and Spread of Yielding**

A proposal for the limit state of ductility of tapered plate columns is made using the experiments carried out at Fukuyama University, Japan [4] and their analytical results [7]. In brief, one uniform (TPRC 9-9) and three LP plate columns (TPRC 9-6, 9-5 and 12-6) were tested under the combined action of an axial compression  $P$  and cyclic lateral loads  $H$  applied to the column top. TPRC 9-6 signifies box column with variable flange and web plate thickness from 9 mm at the base to 6 mm at the end of LP plate. The tapering ratios are  $\eta = 0.0$  (TPRC 9-9), 0.60 (TPRC 9-6), 0.79 (TPRC 9-5), and 0.92 (TPRC 12-6). The height of specimens is 2289 mm and the outer dimension of section at the base is 450 × 450 mm. Tapered plates are used for panels 1 to 3 in LP plate columns. This means, the length of tapered and uniform panels are 1350 and 900 mm, respectively. Cyclic displacement history is a series of quasi-static lateral cyclic displacements at the column top with the peak displacement being increased step-by-step as a multiple of yield displacement of the column. The cyclic history is imposed up to 4 to 5 cycles for maximum horizontal load  $H_{max}$ , and up to 7 to 8 cycles where failure occurs. It was clear from the

observed and analytical hysteretic behavior of specimens that the predicted and test results agreed quite closely up to the maximum load, as is also the case with the other specimens. Fig. 6 shows the measured axial strain  $\varepsilon/\varepsilon_y$  distributions of the specimens along the longitudinal flange-web edge lines of the LP flange plate under  $H_{max}$ . The panels where pronounced local strains occurred at 4 to 5 cycles developed local cyclic buckling at failure. High strain concentration is observed in Panel 1 ( $x/h=0-0.2$ ) of the uniform thickness specimen TPRC 9-9, while averaged larger strain distributions are observed in Panel 2 ( $x/h=0.2-0.4$ ) and Panel 3 ( $x/h=0.4-0.6$ ) for other LP plate specimens depending on the plate tapering ratios.

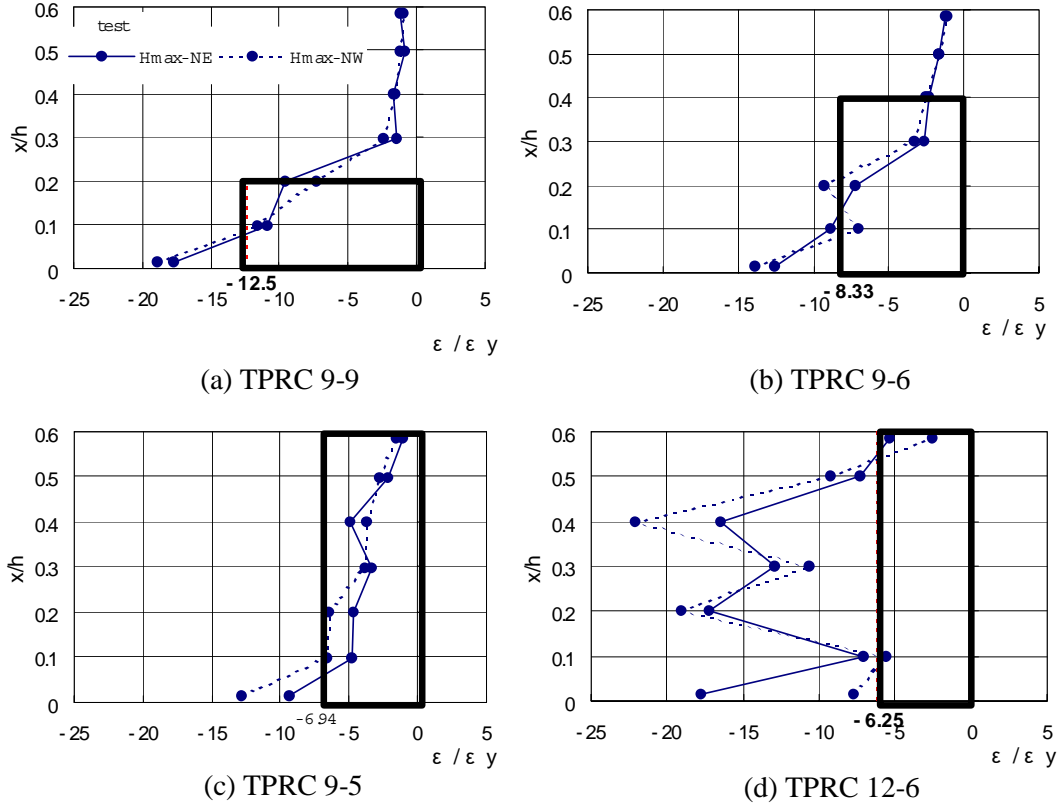


**Fig. 6 Distribution of Axial Strains along the Flange Edges at  $H_{max}$**

The specifications for seismic design of highway bridge piers, JHBS 2002 [1], give a simple empirical relation between the design limit strain,  $\varepsilon_a$ , and the flange slenderness parameter,  $R_F$ , for the bottom panel of the uniform bridge piers having the stiffened rectangular box sections as,

$$\frac{\varepsilon_a}{\varepsilon_y} = 20 - 25R_F \quad (9)$$

where  $\varepsilon_a$  = the design limit strain in the flange plate under the combined action of axial and cyclic horizontal loads applied to the column top, and it is the permissible strain which is obtained from the acceptable limit state of horizontal displacement of the pier at the column top under the maximum horizontal load,  $\varepsilon_y$  = yield strain, and

$$R = \frac{b}{t_f} \sqrt{\frac{\sigma_y}{E} \frac{12(1-\nu^2)}{\pi^2 k}} \quad (10)$$

for  $0.2 \leq R_F \leq 0.5$  and  $0.3 \leq R_R \leq 0.5$ , and  $0 \leq P/P_y \leq 0.2$  and  $\gamma/\gamma^* > 1.0$ , where  $b$  = flange breadth between inside faces of web,  $t_f$  = flange thickness of plate,  $\sigma_y$  = yield stress,  $E$  = modulus of elasticity,  $\nu$  = Poisson's ratio,  $k$  = elastic buckling coefficient of plate in compression, and subscripts  $R$  and  $F$  = local buckling between stiffeners and overall buckling of stiffened plate, respectively. Notation  $P_y$  stand for squash load. Equation (9) can be extended to the LP plate piers as,

$$\frac{\varepsilon_a}{\varepsilon_y} = \{20 - 25 \cdot \max(R_F, R_R)\} \cdot \frac{M_{ycU}}{M_{ycl}} \quad (11)$$

and Eq. (11) can be simply expressed as,

$$\frac{\varepsilon_a}{\varepsilon_y} = \{20 - 25 \cdot \max(R_F, R_R)\} \cdot \frac{t_U}{t_L} \quad (12)$$

by assuming in practical conditions terms  $(1-P^*)$  and  $(1-P^* t_U/t_L)$  in Eqs. (4) and (5) are nearly the same. Flange slenderness parameters  $R_F$  and  $R_R$  are given for the mid-panel sections of panels. The  $\varepsilon_a/\varepsilon_y$  values are calculated by Eq. (12) for  $H_{max}$  and the results are shown in Fig. 6 surrounded by thick lines.

The test deformations of Panels 1, 2, and 3 for the specimens TPRC 9-9 and TPRC 12-6 after test (i.e., unloaded from the 8<sup>th</sup> cycle ( $\pm 8\delta_y$ )) are compared with the predicted ones in Fig. 7, and the predicted deformations at  $H_{max}$  of the 5<sup>th</sup> cycle ( $\pm 5\delta_y$ ) are also shown for comparison. The out-of-plane deflections of flange panel plates correspond to the  $H_{max}$  are difficult to trace, but beyond the 5<sup>th</sup> cycle, the flange panel plates continue to deflect until the test completed. It is obvious from the predicted deformations after the test that the local deformation is concentrated in Panel 1 for TPRC 9-9, while in TPRC 12-6, yielding spreads in Panels 1, 2 and 3 and the localized deformed shapes are considerably small.

## Ductility Assessment

### *Ductility Factor*

The structural member ductility factor  $\mu$ , can be defined as,

$$\mu = \frac{\delta_{max}}{\delta_y} \quad (13)$$

where  $\delta_{max}$  = horizontal displacement at the column top for maximum horizontal load,  $H_{max}$ , and  $\delta_y$  = horizontal yield displacement modified to include the effect of axial compression.

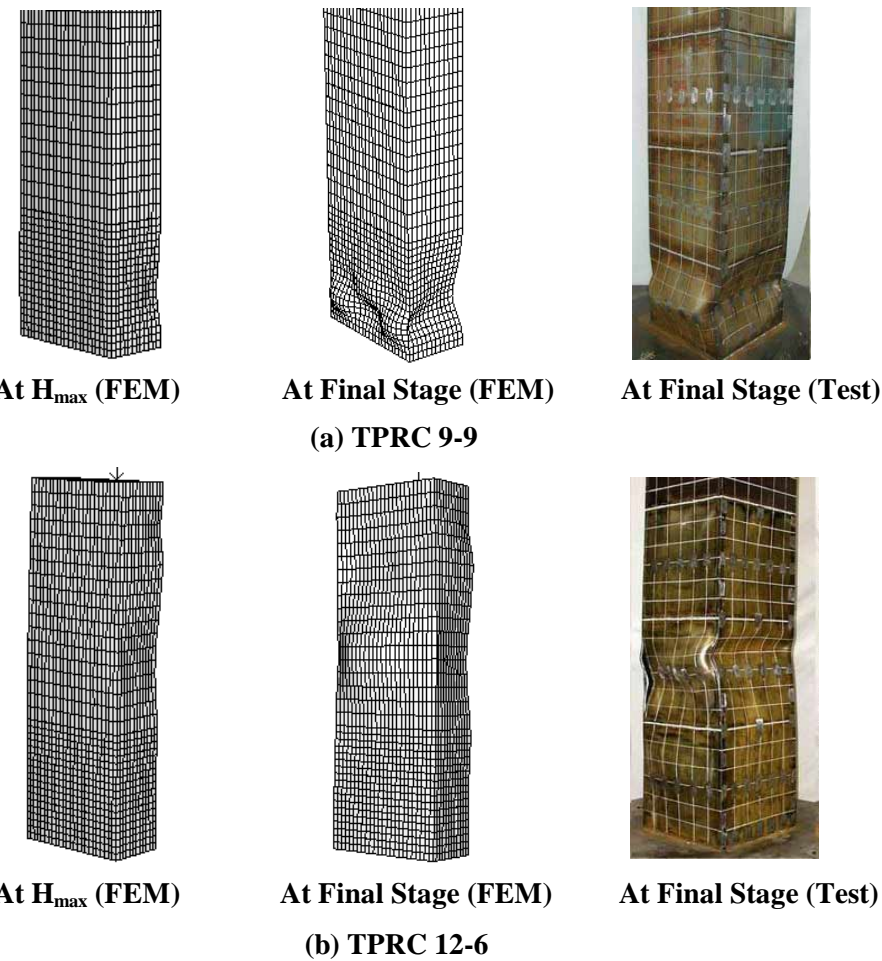


**Fig. 7 Deformed Shapes of Specimens (a) TPRC 9-9; and (b) TPRC 12-6 at  $H_{\max}$  and Final Stage of Test**

**Table 2 Ductility Factor  $\mu$  and Tapering Ratio  $\eta$**

Specimens	FEM Analysis			$\mu$	Rigid-plastic Method			$\eta$
	$\delta_y$ (mm)	$\delta_{\max}$ (mm)	$\mu$		$\delta_y$ (mm)	$\delta_{\max}$ (mm)	$\mu$	
TPRC 9-9	8.5	42.5	5	5	5.4	67.3	12.5	0
TPRC 9-6	9.8	49.0	5	4	9.6	80.0	8.3	0.6
TPRC 9-5	9.9	49.5	5	4	12.3	85.3	6.9	0.79
TPRC 12-6	10.5	63.0	6	5	12.1	75.5	6.2	0.92
TPRC 12-5	10.5	31.5	3	—	—			1.0

A summary of test and analytical results for  $\mu$  with the corresponding tapering ratio  $\eta$  is given in Table 2. As per the analytical results, the amount of  $\delta_{\max}$  of specimen TPRC 12-5 is only a half of  $\delta_{\max}$  of specimen

TPRC 12-6. The specimen TPRC 12-5 which has the tapering ratio  $\eta = 1$  means that the compressive outer flange fibers along the length of the tapered portion reach yielding simultaneously, and as soon as the attainment of  $H_{max}$  the capacity of the specimen begin to deteriorate with further cycles due to the cyclic local buckling in Panel 3. Compared to the specimen TPRC 12-6 which has  $\eta = 0.92$  and LP slope of 4.4 mm/m, the specimen TPRC 12-5 has LP slope of 5.2 mm/m and thus 17 % steeper than the slope of TPRC 12-6. This means it is important to control the plate slope to avoid earlier degrading due to the local plate buckling of thinner plate part.

#### *Rigid-plastic method*

Equation 12 gives the critical strain  $\varepsilon_a$  for the stiffened box columns having LP plates, and the calculated strain results are shown in Fig. 6 surrounded by the thick lines that extend to the yielding zone of the LP plates. The  $\varepsilon_a$  value is kept constant in the yielded zone. Using the  $\varepsilon_a$  value the curvature and then the change in slope between the both ends of the yielded zone can be obtained. Elastic part of the columns is assumed as rigid since taper length is usually half or more than half of the member. The  $\delta_{max}$  values obtained for the specimens are listed in Table 2 in the column of Rigid-plastic method. Value of  $\delta_y$  is obtained when  $\varepsilon_a = \varepsilon_y$ . The rigid-plastic method is simple but effective way to explain the behavior and to estimate the deflection of the column as the constant plastic strain developing over the whole taper plate can bring easy calculation.

## DESIGN AND ANALYSIS OF A RIGID-FRAME PIER

### **Structural Model of a Rigid-Frame Pier**

A large-scale model was fabricated and tested to investigate the failure and collapse mechanism when subjected to a large earthquake. The model consisted of a one-story, rigid-frame pier with a beam length of 5.0 m, a column height of 5.8 m, and a 600×600×6 mm rectangular cross section [11]. Failure originated at the base of the columns and then propagated to the lower portion of the beam-column connection. The frame was modeled using FEM and the prediction corresponds well with the collapse phenomenon of the experimental test. The same large-scale model is used to study the application of LP plates in this study.

### **Design Flow and Arrangement of LP Plates at the Pier**

A step-by-step procedure for arrangement of LP plates in rigid-frame piers are explained as follows:

- 1) Set up of two-way model: A rigid frame pier models are created in longitudinal and transverse directions of the bridge axis.
- 2) Elastic analysis: In the case of loading when subjected both to vertical load (dead load) and horizontal load of earthquake, member forces including  $H_y$  that is the horizontal force when plate at the base yields, are calculated and moment diagram is viewed.
- 3) Estimate of  $H_{max}$  (Ultimate strength at the failure): In general,  $H_{max}$  is estimated by testing or finite element analysis. Experimental results show  $H_{max} = 1.65H_y$  in the transverse direction and 1.6~1.7 $H_y$  in the longitudinal direction. Those values are considered to be smaller when LP plates are used.
- 4) Partitioning of elastic and plastic regions: Three regions are to be considered as:
  - (a) Elastic zone (no buckling occurs) - Use high strength steel with thin plates for cost saving;
  - (b) Plastic zone (failure occurs) - Use LP steel with stiffened thick plates against damages;
  - (c) Boundary zone - For keeping high ductility, discontinuity should be avoided to prevent stress concentration there.
- 5) Two-way arrangements: LP plates are arranged both for flanges and webs considering earthquake loads in both transverse and longitudinal directions. Tapering ratios are sometimes different from each other.

- 6) Concrete casting: Casting height  $h_c$  should be determined so that failure never occurs at the discontinuous sections of the boundary. Length of  $h_c$  should be governed by the condition given in Eq. (1) satisfying longitudinal and transverse direction.

#### Critical Tapering Ratio and its Precise Evaluation

1. Preliminary estimation: Thickness of LP plates is determined so that the critical tapering ratio is satisfied.
2. Thickness  $t_U, t_L$  should be satisfied with the critical tapering ratio.
3. Precise evaluation: The combined stress of LP plates with stiffeners should be calculated precisely at each section and checked whether the stress are within the design criteria. The combined stress at **B** and **C** should be always less than that at **A** (See Fig. 8 for points **A**, **B**, and **C**). Otherwise, failure moves to the weak sections from **A** to **B** and **C**.

Combined stress  $\sigma = \sigma_n$  (due to thrust) +  $\sigma_m$  (due to moment)

- 1) Point **A** (at maximum member forces, M, P, Q): Control point of first yielding
- 2) Point **B** (at minimum member forces, M, P, Q): Discontinuity point between LP and uniform plates where stress concentration occurs.
- 3) Point **C** (at intermediate sections): (1-P/P<sub>y</sub>) effect becomes crucial if thrust is predominant.

#### A Few Feasibility Studies with a Parameter of Tapering Ratios

LP plates are allocated in the plastic regions. On the basis of  $H_{max} = 1.65H_y$ , the lengths of plastic and elastic regions of the rigid-frame are determined according to the above procedure. The bending moment diagram is shown in Fig. 8 and it is used in subsequent FEM analysis presented in following section. The values are presented in Table 3 together with the equivalent thickness of LP plates on the base of original uniform thickness. In the designation of frames, two figures followed by "LP" indicate the maximum and minimum thickness of plates. The length along plastic region times the tapering ratios indicate a cost saving factor of steel weight reduction. In general, LP plates used in piers aim to the cost saving and good seismic performance with approximately the same weight of material.

**Table 3 Parameters of Feasibility Study**

	lp1 (mm)	ep1 (mm)	lp2 (mm)	ep2 (mm)	Equivalent thickness
T=6 mm	1272	1956	616	1956	6
LP 12+6	1272	1956	616	1956	9.96
LP 10+5	1272	1956	616	1956	5.80
LP 9+6	1272	1956	616(1100)	1956(1472)	6.48
h=5800 mm, h1=3228 mm, h2=2572 mm					
H <sub>y</sub> =558 kN, P=0.15P <sub>y</sub> =668 kN, M <sub>y</sub> (base)=904 kN.m M (top)=720 kN.m, H <sub>max</sub> =1.65H <sub>y</sub> =920 kN Elastic region=ep1+ep2, Plastic region=lp1+lp2					

#### FEM Analysis and Results

The rigid frame pier explained in the preceding section was numerically analyzed using large deformation finite element analysis program ABAQUS [12]. The analyses were carried out for original test frame and three cases presented in Table 3. The model consists of combination of four-nodes doubly curved shell element (S4R), four-node liner beam-column element (B31OSH) and rigid beam elements (R2D2) available in the program. Only a half of the frame is modeled due to the symmetry in loading and the geometry. The element mesh is shown in Fig. 9. As seen in the figure, the mid portion of the columns are

modeled using beam-column elements while shell elements are employed at the vicinity of the base and joints. Mesh size is decided based on a trial and error method. The length between the base and the first diaphragm is divided into 18 segments while subsequent each length is divided into 6 segments. Each subpanel between longitudinal stiffeners consists of 4 columns of shell elements. Three (3) columns of elements are assigned in longitudinal stiffeners. The thickness of shell elements representing the tapered plates were defined by assigning the appropriate nodal thickness. Rigid beam elements are used at the interface between shell elements and beam-column elements as well as at the joints. This kind of modeling greatly improves the efficiency of the analysis while maintaining the accuracy of the solution. The material behavior of shell elements was simulated by the modified two surface plasticity model (2SM) [13]. A bilinear elasto-plastic model was used to simulate the material behavior of beam-column elements.

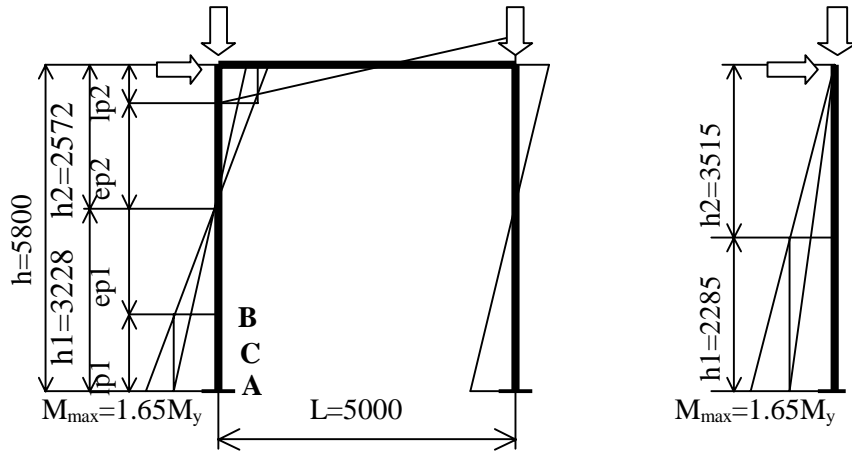


**Fig. 8 Rigid-Frame Pier Model**

Cyclic lateral loads are applied in terms of stepwise yield displacements at the top left corner of the model. For known yield load, corresponding displacement for each frame is decided by the results of pushover analysis and subsequently used it as yield displacement. For a better comparison, envelope curves of load-displacement hysteretic behavior for all the cases are presented in a one plot as shown in Fig. 10.

It is clear from this figure that the strength and ductility performance of LP 12+6 and LP 9+6 are far better than those of constant thickness plate frame. Obviously frame LP 12+6 should show higher strength as it utilize larger amount of steel than constant thickness frame. The frame LP 10+5 shows almost equal strength but ductility seems

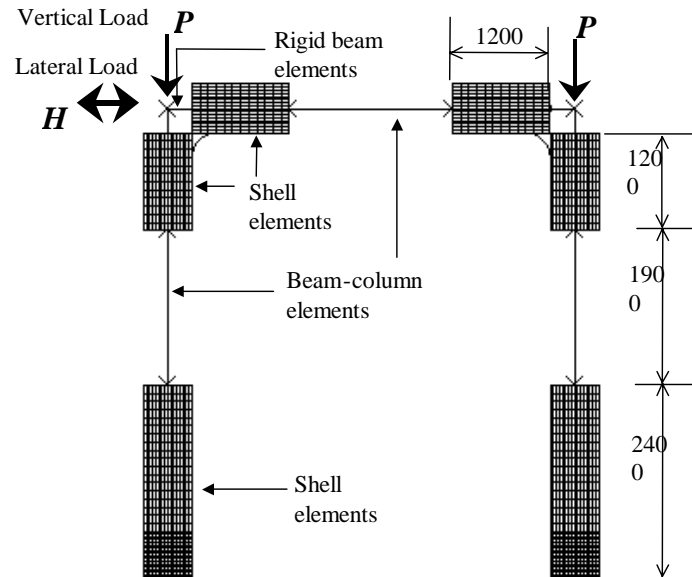


**Fig. 9 FEM Model**

to be improved. Frames LP 10+5 and LP 9+6 use approximately the same amount of steel as constant thickness frame. So, it is clear from the results that the use of tapered plates in frame type structures improves the strength and ductility performance when proper tapering ratio is provided.

### Design Flow Chart for Steel Pier with LP Plates

Steps in design of steel piers using LP plates are summarized in the flow chart given in Fig. 11.

### CONCLUSIONS

In this paper, fundamentals in application of LP plates in steel columns, and the performance assessment of LP plate columns were presented based upon the several laboratory experiments and analytical works. Also, a design proposal was made for application of LP plates in steel piers in highway bridge systems. The main conclusions of this study are:

1. Optimum tapering ratio can lead to larger spread of yielding in the LP plate panels and to contribute significantly to the cyclic performance of the columns. However, earlier degradation due to the local buckling of the thinner parts of panels can be avoided by limiting the plate slenderness parameters of the flange plates.
2. A spread of yielding in the LP plate panels can reduce an excessive concentration of the out-of-plane deformation in the panel zones and thus reduce the need for urgent repair work after an earthquake.
3. A comparison of LP plate columns and uniform thickness plate column in which the thickness is equal to the equivalent LP plate thickness shows that a better performance of ductility and energy dissipation can be obtained from the LP plate columns.
4. The analytical results of portal frames indicate that the use of LP plate panels at the both ends of the columns can improve the strength and ductility of the frames under cyclic horizontal loading.
5. A seismic design method is proposed for the portal frames using LP plates at the both ends of columns.

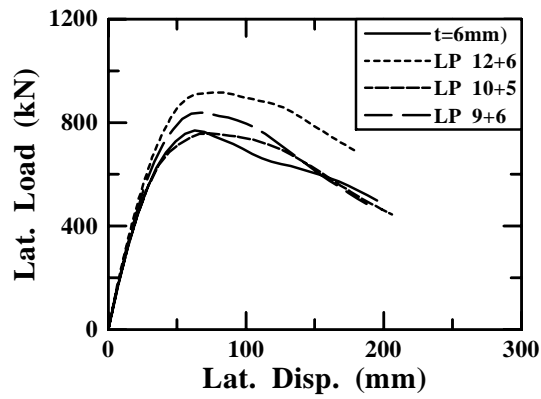


**Fig. 10 Lateral Load-Displacement Envelope Curves**

**Step-1:-**Original design of piers: Ordinary design with uniform Plates.

**Step-2:-**Set up two models: In longitudinal and transverse directions.

**Step-3:-**Partitioning elastic, plastic regions and boundary zones: Rough planning of use of LP plates

**Step-4:-**Estimate of  $H_y$  and  $H_{max}$  (Ultimate strength at the failure): By experimental data.

**Step-5:-**LP plates design step 1 (Preliminary estimation): Thickness is determined by satisfying optimum tapering ratio.

**Step-6:-**LP plates design step 2 (Precise evaluation): Combined stresses are checked at each critical section of LP plates with stiffeners.

**Step-7:-**FEM analysis: Strength and ductility are evaluated whether the performance assessment is established.

**Fig. 11 Design Flow Chart**

## ACKNOWLEDGEMENT

The experimental investigation referred in this paper has been conducted at Fukuyama University and Aichi Institute of Technology, Japan. The writers wish to express their sincere gratitude to the group members who have conducted the experimental works.

## REFERENCES

1. Japan Specification for Highway Bridges, Part V: Seismic Design, 2002.
2. Hotta T, Tani T, Kudo J, Nishimura N. "Application of Longitudinally Profiled Steel Plate to Steel Bridges." *J. Bridge and Foundation*, 2000, 11-14 (In Japanese).
3. JFE Catalog. "JFE LP Plates." JFE Steel, Cat.No.C1J-014-00.
4. Fukumoto Y, Uenoya M, Nakamura M, Saya H. "Cyclic Performance of Stiffened Square Box Columns with Thickness Tapered Plates." *J. Steel Structures*, 2003; 3: 107-115.
5. Uenoya M, Nakamura M, Fukumoto Y, Yamamoto S. "An Experimental Study on the Elastic-Plastic Hysteretic Behavior of Tapered Box Columns." *J. Steel Construction Engineering, JSSC*, 2002; 9(33): 25-35 (in Japanese).
6. Uenoya M, Nakamura M, Fukumoto Y, Yamamoto S. "Cyclic Performance of Square Box Columns with Thickness Tapered Plates." *J. Structural Engineering, JSCE*, 2003; 49A: 115-125 (in Japanese).
7. Fukumoto Y. "Cyclic Performance Assessment of Stiffened Box Columns with Thickness Tapered Plates." Proceeding of SSRC Annual Technical Sessions & Meeting, Long Beach, 2004.
8. Kumano T, Tukamoto Y, Hiroe A, Aoki T. "Experimental Study (1) on Seismic Performance of Steel Piers with LP plates (Mold line and Tapering Ratio)." Proceeding of the Annals of JSCE, 2003; No.58 (in Japanese).
9. Yamamoto R, Aoki T, Kumano T, Tukamoto Y. "Experimental Study (2) on Seismic Performance of Steel Piers with LP plates(Stiffeners and Tapering Ratio)." Proceeding of the Annals of JSCE, 2003; No.58 (in Japanese).
10. Takaku T, Aoki T, Matsuda H, Nakajima I, Kumano T. "Cyclic Loading Test of Square Box Column with LP Plates." Proceeding of the Annals of JSCE, 2002, No.57 (In Japanese).
11. Nishikawa K, Josen Y, Takahashi M, Takaku T. "Experimental Study on Failure and Collapse of Rigid-Frame Piers of Highway Bridges." Proceeding of the 14<sup>th</sup> US-Japan Bridge Engineering Workshop: PWRI, Pittsburgh, 1998.
12. ABAQUS User's Manual-version 6.4. (2003). ABAQUS, Inc., Pawtucket, R. I.
13. Shen C, Mamaghani IHP, Mizuno E, Usami T. "Cyclic behavior of structural steels." *J. Structural Engineering, ASCE*, 1995; 121(11), 1165-1172.